Progress In Electromagnetics Research C, Vol. 64, 61–70, 2016

A Compact Dual-Band Dual-Polarized Antenna for Base Station Application

Guanfeng Cui[1, *], Shi-Gang Zhou[2], Gang Zhao[1], and Shu-Xi Gong[1]

Abstract—A compact dual-band dual-polarized antenna is proposed in this paper. The two pair dipoles with strong end coupling are used for the lower frequency band, and cross-placed patch dipoles are used for the upper frequency band. The ends of the dipoles for lower frequency band are bent to increase the coupling between adjacent dipoles, which can benefit the compactness and bandwidth of the antenna. Breaches are introduced at the ends of the dipoles of the upper band, which also benefit the compactness and matching of the antenna. An antenna prototype was fabricated and measured. The measured results show that the antenna can cover from 790 MHz to 960 MHz (19.4%) for lower band and from 1710 MHz to 2170 MHz (23.7%) for upper band with VSWR < 1.5. It is expected to be a good candidate design for base station antennas.

1. INTRODUCTION

With the rapid development of mobile communication systems, multiple communication standards exist simultaneously in a cellular radio network. Since the site for construction of base station antenna is a rare resource, a base station antenna is expected for broad and multi-band. A dual-polarized antenna can decrease fast fading of the signal and increase system capacity [1]. Therefore, a dual-band dual-polarized antenna with small size can bring enormous convenience to the construction of base station antennas.

Many researchers have made a lot of efforts on the development of dual-polarized antennas [2–13] and broadband base station antennas [8–10]. The dual-band dual-polarized antenna that proposed in [6] was formed by arc-probe-fed annular ring element and pairs of cross microstrip dipoles nested together, and achieved an impedance bandwidths of 17.4% (806 $\sim$ 960 MHz) for VSWR < 2 in the lower band and 23.7% (1710 $\sim$ 2170 MHz) in the upper band, respectively. The stacked patch antenna that proposed in [2] was fed by aperture coupling structure and had an impedance bandwidth of 20.4% (790 $\sim$ 960 MHz) with VSWR < 1.5 in the lower band and 29.3% (1630 $\sim$ 2190 MHz) with VSWR < 1.6 in the upper band, respectively. Both of the above mentioned antennas have complex feeding structures and high mass production cost.

In this paper, a compact, dual-band and dual-polarized antenna for base station application is proposed based on the work in [7]. The proposed antenna achieves a bandwidth of 19.4% ranging from 790 MHz to 960 MHz with VSWR < 1.5 and 23.7% ranging from 1710 MHz to 2170 MHz with VSWR < 1.5, respectively. The simulated and measured results show that the proposed antenna has good impedance and radiation pattern performances, and can be a good candidate for mobile communication base station applications.

Received 2 April 2016, Accepted 7 May 2016, Scheduled 13 May 2016

* Corresponding author: Guanfeng Cui (cuigf@mail.xidian.edu.cn).

[1] National Key Laboratory of Science and Technology on Antennas and Microwaves, Xidian University, Xi'an, Shaanxi 710071, China.

[2] School of Electronics and information, Northwestern Polytechnical University, Xi'an 710072, China.

2. ANTENNA CONFIGURATION AND DESIGN

The configuration of the proposed antenna is illustrated in Fig. 1 and Fig. 2. The proposed antenna consists of a lower band element, upper band element, metal reflector and square metal baffle. The upper band element nested in the center of the lower band element.

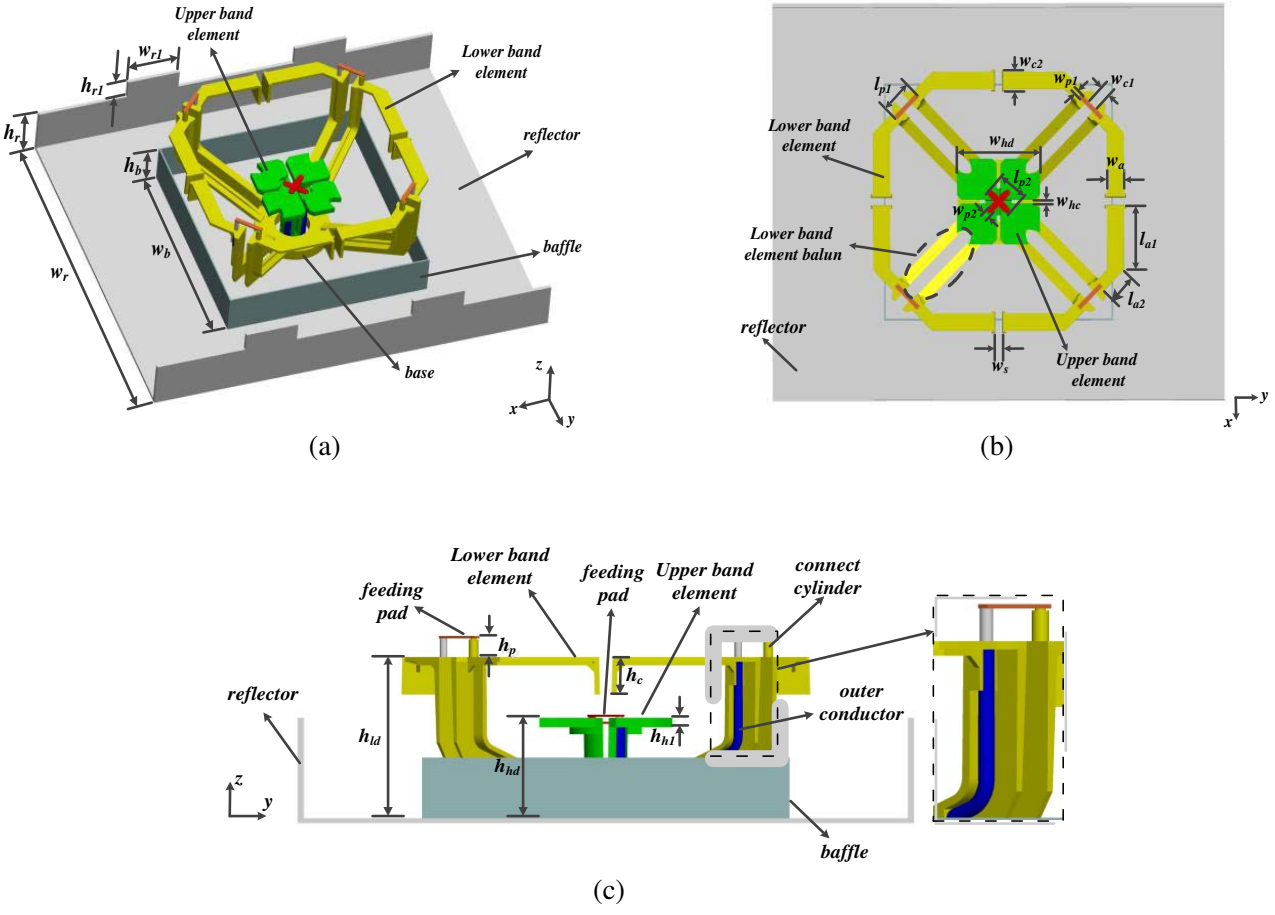

(a) (b) (c)

Figure 1. Geometry of the proposed antenna. (a) 3D view. (b) Top view. (c) Side view.

2.1. Design of the Lower Band Element

The lower band element of the antenna was proposed in [7], which consists of four dipoles, four baluns and one base. Among the four dipoles, the two opposite dipoles which have the same polarization direction are combined to form one polarization of the element. The dipoles are fed directly by coaxial cables and metal feeding pads. The outer conductors of the coaxial cables are soldered with the balun, which provide balanced feeding to the element (as seen in Fig. 1(c)). As shown in Fig. 1, the arms of the dipole are designed with bent shape to reduce the size of the antenna.

2.2. Design of the Upper Band Element

As illustrated in Fig. 2, the upper band element of the antenna consists of two cross patch dipoles, an integrated balun and two metal feeding pads. The two cross patch dipoles are fed directly by the feeding pads and coaxial cables, which have a simple and stable feeding structure. The cross patch dipole has

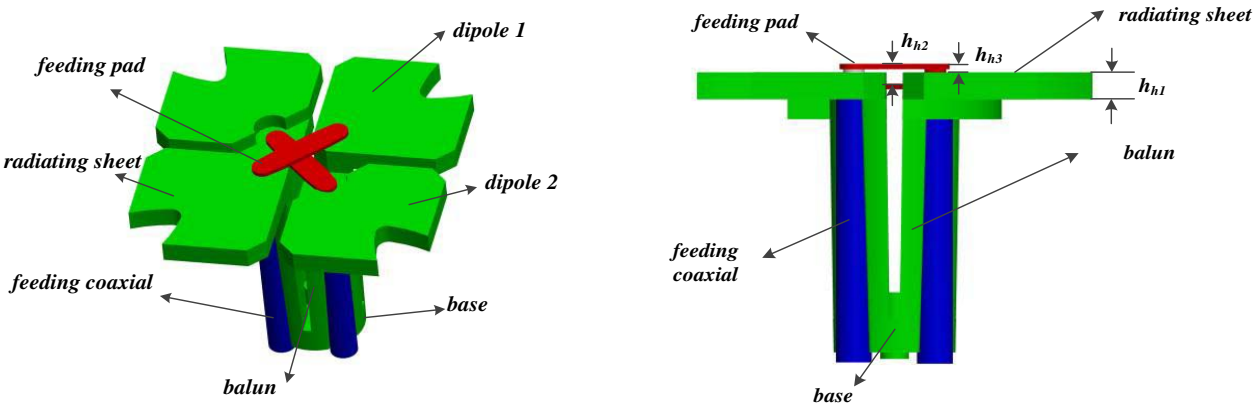

Figure 2. Perspective view of the upper band element of the proposed antenna. (a) 3D view. (b) Top view. (c) Side view.

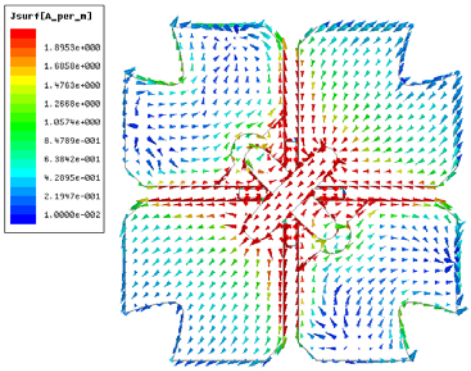

Figure 3. Current vector distribution on the element of 1940 MHz when only dipole 1 is fed.

two arms made up of square metal sheets. The arms connect with the top end of the balun. The baluns of the two polarizations are combined at the bottom end and electrically connected with the reflector below. The outer conductor of the cable used to feed the dipole is soldered with the balun, while the inner conductor of the cable is soldered with the pad which is connected to the other arm of the dipole. The balun can provide a balanced feed for the dipoles and also support the arms of the dipoles.

Figure 3 shows the current vector distribution of 1940 MHz on the element when only dipole 1 is fed. Due to dipole 2 and the strong coupling between the crossed dipoles, the excited currents on dipole 1 flow mainly along the edges of the square metal arms of the dipole, which is useful to extend the flowing path of the current and then reduce the size of the antenna. The strong coupling can also extend the bandwidth of the antenna, and the principle is similar to that in [10].

By changing the width of the feeding pads, the impedance characteristic of the upper band element can be adjusted, which is illustrated in Fig. 4. When parameter w_{p2} is studied, the other dimensions of the element are as the parameters listed in Table 2. With the increase of w_{p2}, the VSWR at low end of the frequency band becomes worse. However, if w_{p2} is too small ($w_{p2} = 3.5$), the VSWR at the high end of the frequency band will become worse. Finally, parameter w_{p2} is optimized with the value of 4.4 mm to achieve the best VSWR result. The two orthogonal feeding pads are located with a distance in height to avoid interference in mechanism. To improve the impedance characteristic of the dipoles, the four square metal sheets have been cut at the corners, which also benefit the compactness of the antenna. Fig. 5 shows the influence of the cut to the VSWRs of the element. It is seen that with the cut in the corner, the VSWRs of the element become better over the whole operating frequency band.

2.3. Design of the Reflector and the Square Baffle

To achieve directional radiation pattern, a metal reflector is added for the antenna. The size of the reflector is mainly determined by the radiation characteristic of the lower band element. The design of two crenellated side walls of the reflector is needed to improve the front-to-back ratio of the antenna radiation patterns in the lower band.

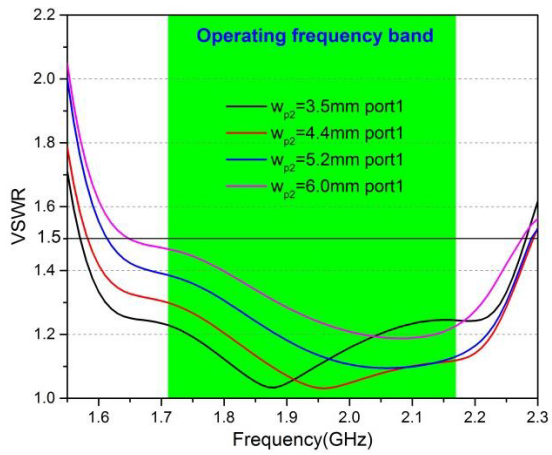

Figure 4. Simulated VSWR, varying w_{p2} (width of the feeding pad).

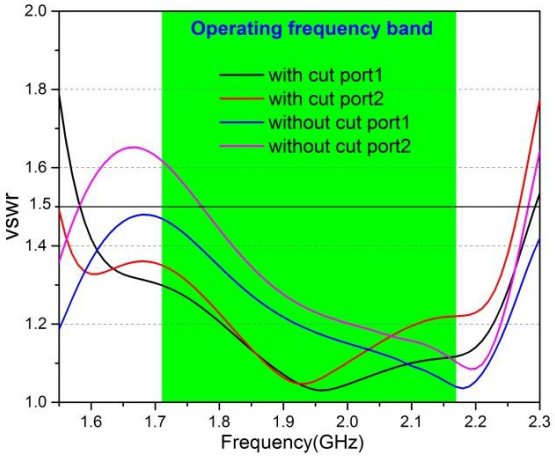

Figure 5. Influence of the cut to the VSWRs of the upper element.

Table 1. The influence of the square metal baffle on the radiation characteristic of the upper band element of the antenna.

Frequency (MHz)	Without square metal baffle			With square metal baffle		
	Gain (dBi)	HPBW	Front-to-back Ratio (dB)	Gain (dBi)	HPBW	Front-to-back Ratio (dB)
1710	9.89	64.9	23.8	9.42	65.8	26.8
1940	9.54	68.3	28.9	9.36	70.1	28.4
2170	7.89	79.5	26	9.48	62.1	25.1

Table 2. Optimized geometric parameters of the proposed antenna element.

Parameter	Value	Parameter	Value
w_r	255 mm	h_r	32 mm
w_b	152 mm	h_b	26 mm
w_{r1}	39.3 mm	h_{r1}	13 mm
w_s	5.7 mm	w_a	11 mm
l_{a1}	41 mm	l_{a2}	24.3 mm
w_{c1}	7 mm	w_{p1}	3 mm
l_{p1}	20.8 mm	w_{c2}	13 mm
w_{p2}	4.4 mm	l_{p2}	20 mm
w_{hd}	55 mm	w_{hc}	2.5 mm
h_{ld}	71 mm	h_{hd}	45 mm
h_{h1}	4 mm	h_c	16 mm
h_p	9 mm		

The mutual coupling that exists between the upper and lower band elements greatly affects the radiation performance of the upper band element. Seen from the measured results listed in Table 1, the radiation characteristic of the upper band element is improved by adding a square metal baffle around the element. The half-power beamwidth and gain of the upper band element at frequency 2170 MHz change from 79.5° to 62.1° and 7.89 dBi to 9.48 dBi, respectively. The size of the square metal baffle is 150 mm × 150 mm × 26 mm. Optimal geometric parameters of the whole antenna are listed in Table 2.

3. EXPERIMENTAL RESULTS AND DISCUSSION

The proposed antenna is simulated and optimized by Ansoft HFSS 15.0 software, which is based on the finite element method (FEM). To verify the design method, a prototype of the proposed dual-band dual-polarized antenna was fabricated and tested. The fabricated antenna is illustrated in Fig. 6. The two operating elements of the proposed antenna are fed respectively. The upper band element is fed by 50 Ohms cables, while the dipoles of the lower band element are fed by 100 Ohms cables. Then the two 100 Ohms cables combined to match 50 Ohms cables. The S-parameters of the proposed antenna were measured by Agilent E5071C network analyzer in an indoor anechoic chamber. The radiation patterns of the proposed antenna were tested by the far-field test system.

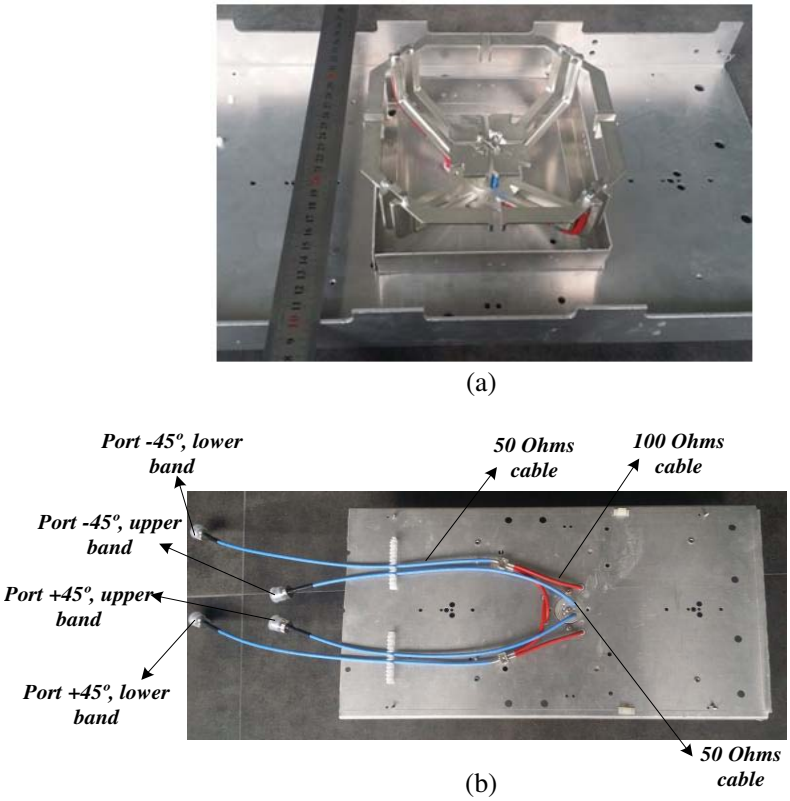

Figure 6. Photograph of the fabricated antenna. (a) Topside view. (b) Backside view.

The comparison of the simulated and measured VSWRs and isolations of the proposed antenna versus frequency are illustrated in Fig. 7 and Fig. 8, respectively. Both the measured and simulated VSWRs of both ports are less than 1.5 in the lower band (790 ∼ 960 MHz, 19.4% bandwidth) and upper band (1710 ∼ 2170 MHz, 23.7% bandwidth), and they agree well with each other. The isolation between +45° and 45° polarizations is sensitive to the deviation caused by manufacture or assembly of the antenna. Both the simulated and measured isolations between the two ports are higher than 26 dB in the lower band and 28 dB in the upper band, respectively. The proposed antenna has a good impedance characteristic to form an array antenna.

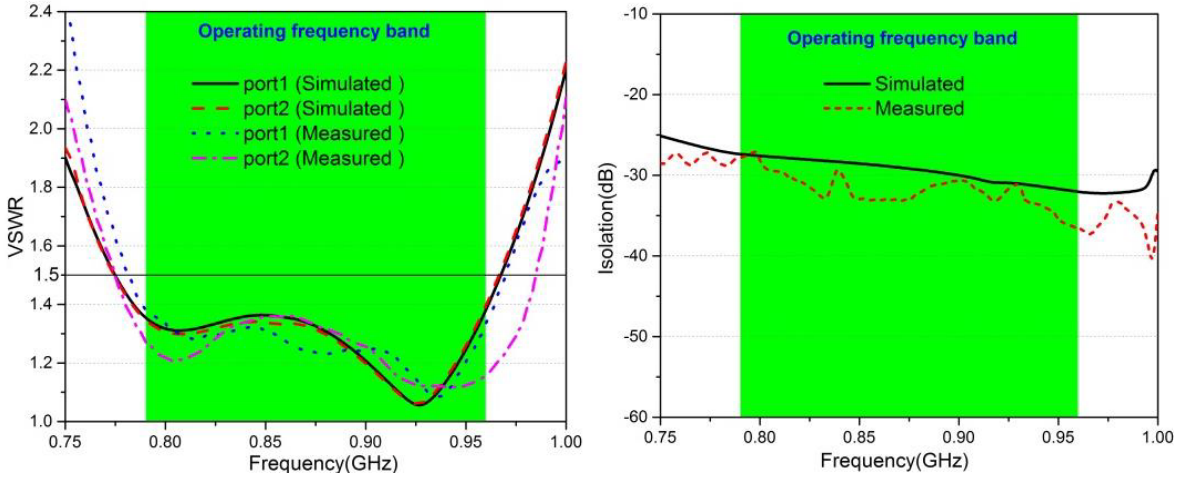

(a) (b)

Figure 7. Simulated and measured VSWR and isolation of the lower band element of the proposed antenna. (a) VSWR. (b) Isolation.

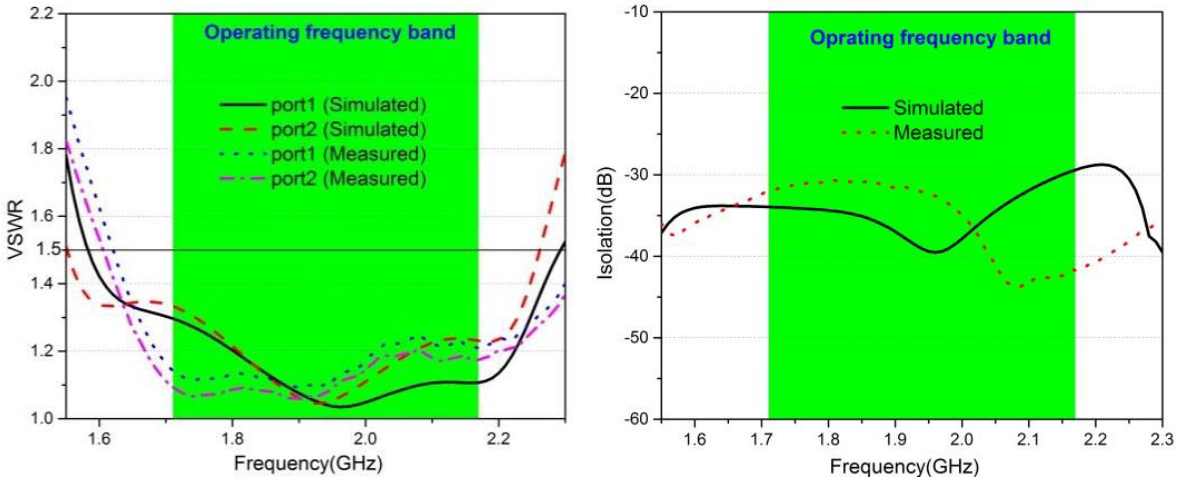

(a) (b)

Figure 8. Simulated and measured VSWR and isolation of the upper band element of the proposed antenna. (a) VSWR. (b) Isolation.

Due to high symmetry of the two polarizations of the proposed antenna, only the radiation patterns of +45° polarization element are presented here. The radiation patterns of the lower band element at the frequencies of 790, 880, and 960 MHz are illustrated in Fig. 9. In the application of base station antenna, the H-planes for the antenna usually refer to the horizontal plane ($\varphi = 90°$), and the E-planes refer to the vertical plane ($\varphi = 0°$). Fig. 10 shows the radiation patterns of the upper band element at the frequencies of 1710, 1940, and 2170 MHz. Most of the measured results agree well with the simulated ones. Due to the existence of the testing error, the radiation patterns of the cross-polarization of the antenna in both bands have some discrepancies between the simulated and measured results.

Figure 11 shows the simulated and measured realized gains and measured half-power beamwidth (HPBW) of the proposed antenna versus frequency at both bands. Table 3 and Table 4 list the radiation parameters extracted from the radiation patterns. The HPBW at H-plane varies from 62.8° to 66.3° in the lower band and from 65.2° to 67.0° in the upper band. The measured gain varies from 9.35 dBi to 9.43 dBi in the lower band and from 9.02 dBi to 9.17 dBi in the upper band. On the other hand,

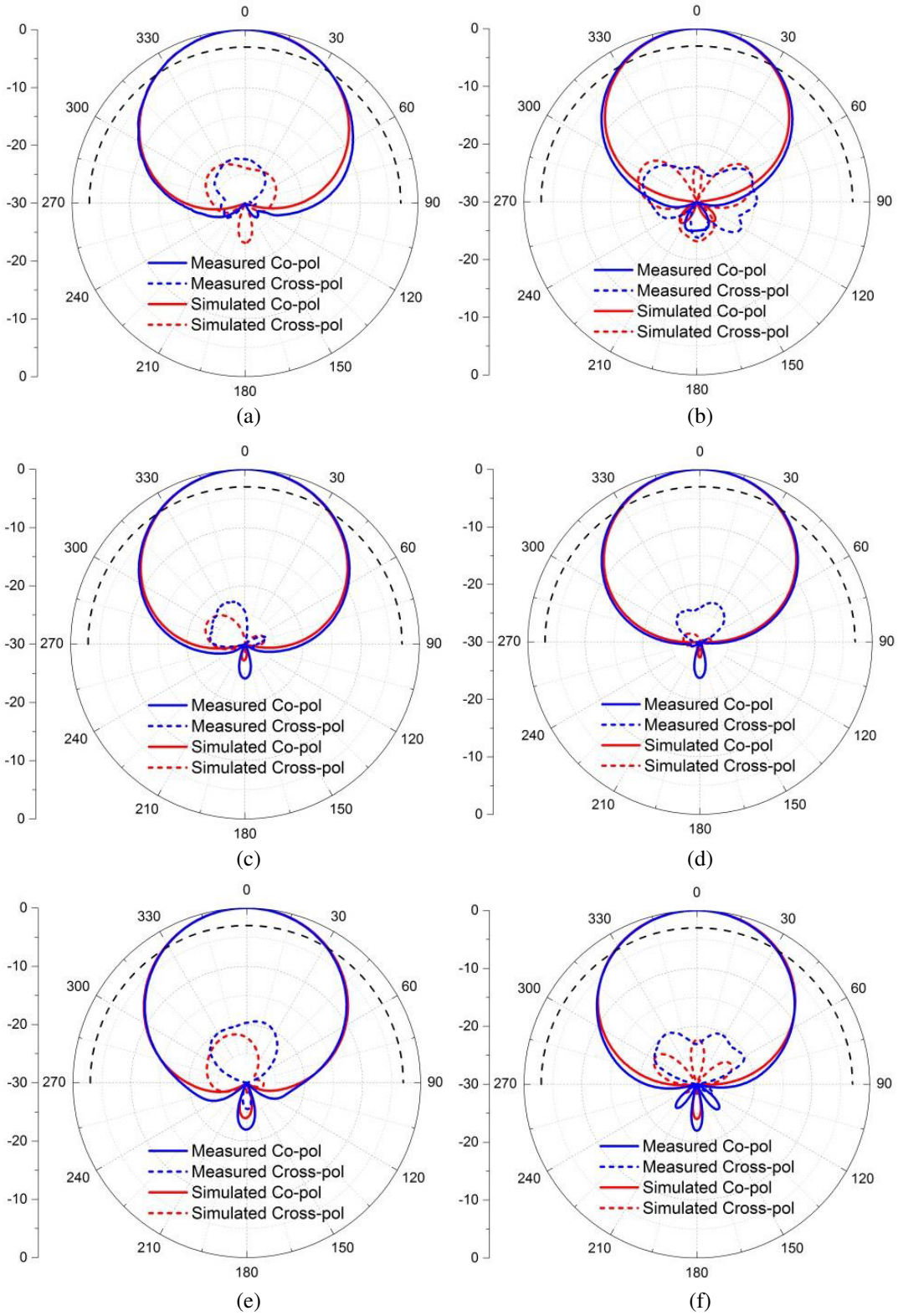

Figure 9. The radiation patterns of the lower band element. (a) 790 MHz H-plane. (b) 790 MHz E-plane. (c) 880 MHz H-plane. (d) 880 MHz E-plane. (e) 960 MHz H-plane. (f) 960 MHz E-plane.

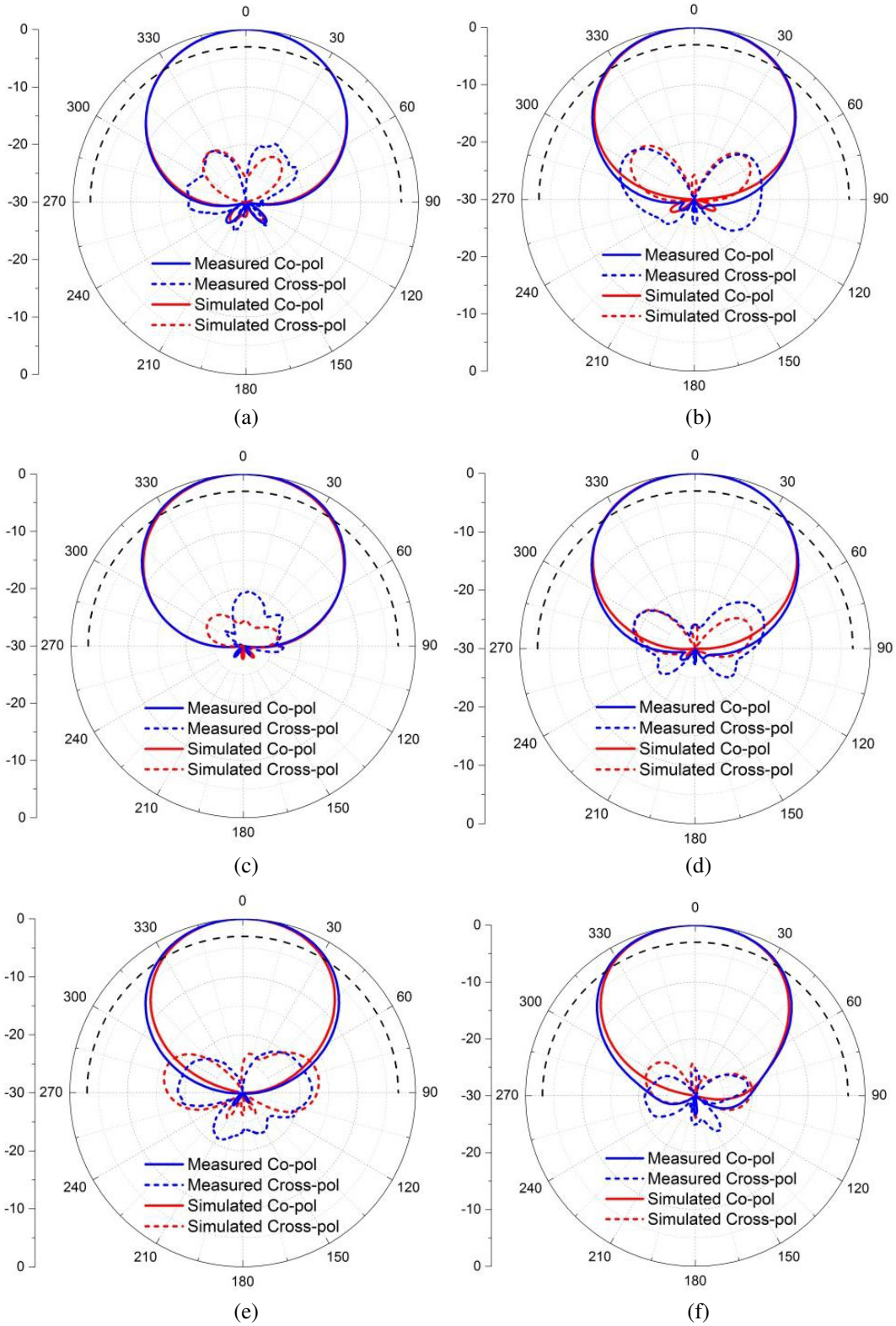

Figure 10. The radiation patterns of the upper band element. (a) 1710 MHz H-plane. (b) 1710 MHz E-plane. (c) 1940 MHz H-plane. (d) 1940 MHz E-plane. (e) 2170 MHz H-plane. (f) 2170 MHz E-plane.

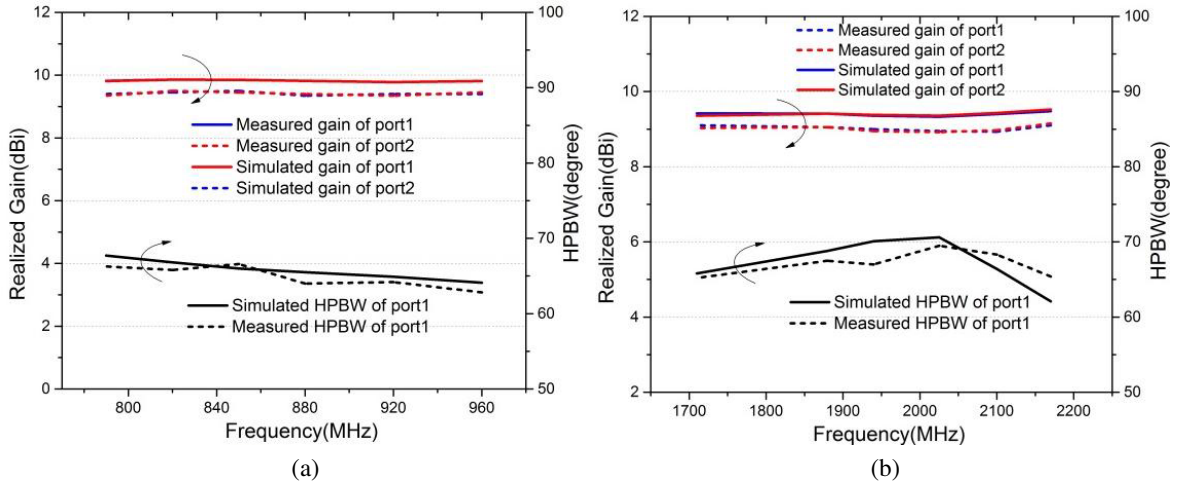

Figure 11. Simulated and measured realized gain and HPBW of the proposed antenna. (a) Lower band. (b) Upper band.

Table 3. Simulated and measured half power beamwidths of the proposed antenna.

Half-power Beamwidth	H-plane		E-plane	
	Simulated	Measured	Simulated	Measured
790 MHz	67.7°	66.3°	56.8°	57.9°
880 MHz	65.5°	64.0°	61.2°	63.4°
960 MHz	64.1°	62.8°	63.9°	62.5°
1710 MHz	65.8°	65.2°	68.4°	69.6°
1940 MHz	70.1°	67.0°	70.0°	69.7°
2170 MHz	62.1°	65.4°	66.6°	69.8°

Table 4. Simulated and measured parameters of the radiation patterns of the proposed antenna.

Frequency (MHz)	Gain (dBi)		Front-to-back ratio (dB) Co (180° ± 30°)		Front-to-back ratio (dB) Cross (180° ± 30°)		Cross polar ratio (dB) 0°	
	Sim.	Mea.	Sim.	Mea.	Sim.	Mea.	Sim.	Mea.
790	9.82	9.43	32.1	27.9	23.2	28.67	23.9	22.4
880	9.82	9.35	27.2	24.1	28.7	32.0	30.0	24.4
960	9.81	9.41	23.9	22.0	28.5	25.5	21.7	19.7
1710	9.42	9.10	26.8	26.3	29.8	24.5	25.7	28.0
1940	9.36	9.02	28.7	27.7	28.4	29.8	25.7	20.7
2170	9.48	9.17	28.6	28.3	25.1	21.0	25.2	28.8

the simulated gain of the antenna varies from 9.81 dBi to 9.82 dBi in the lower band and from 9.36 dBi to 9.48 dBi in the upper band. The measured gain is slightly lower than the simulated result due to losses from the connector and coaxial cables used for testing. The front-to-back ratios of the co- and cross-polarizations are both larger than 22 dB in the lower band and 21 dB in the upper band. The measured cross-polarization level at boresight is 19.7 $\sim$ 24.4 dB lower than the co-polarization level in the lower band and 20.7 $\sim$ 28.8 dB in the upper band.

4. CONCLUSION

A compact, dual-band and dual-polarized antenna for base station application is proposed. The proposed antenna achieves a bandwidth of 19.4% ranging from 790 MHz to 960 MHz and 23.7% ranging from 1710 MHz to 2170 MHz with VSWR < 1.5. The measured isolation between $+45°$ and $-45°$ polarizations in lower and upper bands is larger than 26 dB and 28 dB, respectively. The measured results show that the proposed antenna has good radiation performance including good convergence of HPBW ($65° \pm 3°$ in lower band, $65° \pm 5°$ in upper band), high gain ($9.35 \sim 9.41$ dBi in lower band, $9.02 \sim 9.17$ dBi in upper band), and high front-to-back ratio (> 22 dB in lower band, > 21 dB in upper band). The proposed antenna also has a simple and stable structure, which is beneficial to realizing mass manufacture.

REFERENCES

1. Vaughan, R. G., "Polarization diversity in mobile communications," *IEEE Transactions on Vehicular Technology*, Vol. 39, 177–186, 1990.
2. Kaboli, M., M. S. Abrishamian, S. A. Mirtaheri, et al., "High-isolation XX-polar antenna," *IEEE Transactions on Antennas and Propagation*, Vol. 60, 4046–4055, 2012.
3. Sharma, D. K., S. Kulshrestha, S. B. Chakrabarty, et al., "Shared aperture dual band dual polarization microstrip patch antenna," *Microwave and Optical Technology Letters*, Vol. 55, 917–922, 2013.
4. Gou, Y., S. Yang, Q. Zhu, et al., "A compact dual-polarized double E-shaped patch antenna with high isolation," *IEEE Transactions on Antennas and Propagation*, Vol. 61, 4349–4353, 2013.
5. Chiou, T. W. and K. L. Wong, "A compact dual-band dual-polarized patch antenna for 900/1800-MHz cellular systems," *IEEE Transactions on Antennas and Propagation*, Vol. 5, 1936–1940, 2003.
6. Liu, X., S. He, H. Zhou, et al., "A novel low-profile, dual-band, dual-polarization broadband array antenna for 2G/3G base station," *International Conference on Wireless, Mobile and Multimedia Networks*, 1–4, 2006.
7. Cui, G.-F., S.-G. Zhou, S.-X. Gong, and Y. Liu, "A compact dual-polarized antenna for base station application," *Progress In Electromagnetics Research Letters*, Vol. 59, 7–13, 2016.
8. Cui, Y. H., R. L. Li, and H. Z. Fu, "A broadband dual-polarized planar antenna for 2G/3G/LTE base stations," *IEEE Transactions on Antennas and Propagation*, Vol. 62, 4836–4840, 2014.
9. Liu, Y., H. Yi, F. W. Wang, and S. X. Gong, "A novel miniaturized broadband dual-polarized dipole antenna for base station," *IEEE Antennas and Wireless Propagation Letters*, Vol. 12, 1335–1338, 2013.
10. Bao, Z. D., Z. P. Nie, and X. Z. Zong, "A novel broadband dual-polarization antenna utilizing strong mutual coupling," *IEEE Transactions on Antennas and Propagation*, Vol. 62, 450–454, 2014.
11. Moradi, K. and S. Nikmehr, "A dual-band dual-polarized microstrip array antenna for base stations," *Progress In Electromagnetics Research*, Vol. 123, 527–541, 2012.
12. Peng, H. L., W. Y. Yin, J. F. Mao, et al., "A compact dual-polarized broadband antenna with hybrid beam-forming capabilities," *Progress In Electromagnetics Research*, Vol. 118, 253–271, 2011.
13. Dai, X.-W., T. Zhou, and G.-F. Cui, "Dual-band microstrip circular patch antenna with monopolar radiation pattern," *IEEE Antennas and Wireless Propagation Letters*, 2015.